International Journal of Heat and Mass Transfer 54 (2011) 3970–3978

Contents lists available at ScienceDirect

International Journal of Heat and Mass Transfer

journal homepage: www.elsevier.com/locate/ijhmt

Viscous flow in variable cross-section microchannels of arbitrary shapes

M. Akbari [a,*], D. Sinton [b], M. Bahrami [a]

[a] Mechatronic Systems Engineering, School of Engineering Science, Simon Fraser University, Surrey, BC, Canada V3T 0A3
[b] Department of Mechanical Engineering, University of Victoria, Victoria,BC, Canada V8W 2Y2

ARTICLE INFO

Article history:
Received 9 October 2010
Received in revised form 11 April 2011
Available online 14 May 2011

Keywords:
Slowly-varying microchannels
Arbitrary cross-section
Pressure drop
Modeling
Characteristic length scale
Inertial effect
Frictional effect

ABSTRACT

This paper outlines a novel approximate model for determining the pressure drop of laminar, single-phase flow in slowly-varying microchannels of arbitrary cross-section based on the solution of a channel of elliptical cross-section. A new nondimensional parameter is introduced as a criterion to identify the significance of frictional and inertial effects. This criterion is a function of the Reynolds number and geometrical parameters of the cross-section; i.e., perimeter, area, cross-sectional polar moment of inertia, and channel length. It is shown that for the general case of arbitrary cross-section, the cross-sectional perimeter is a more suitable length scale. An experimental investigation is conducted to verify the present model; 5 sets of rectangular microchannels with converging–diverging linear wall profiles are fabricated and tested. The collected pressure drop data are shown to be in good agreement with the proposed model. Furthermore, the presented model is compared with the numerical and experimental data available in the literature for a hyperbolic contraction with rectangular cross-section.

1. Introduction

The concept of flow through microchannels with gradually varying walls forms the basis of a class of problems in microfluidics which has applications in micromixer design [1–5], accelerated particle electrophoresis [6,7], heat transfer augmentation in micro heat sinks [8–10], flow through porous media [11–15], blood flow in the context of biomechanics [16], preconcentration and separation of molecules [17–19], and polymer processing [20,21]. In most of these applications, it is required to obtain a reasonable estimate of the pressure drop in the channel for basic design and optimization. As a result, pressure drop in microconduits with variable cross-sections has been the subject of several investigations; examples are [2,16,22–29].

A simple model to approximate the flow in a variable cross-section microchannel is to assume that the fluid flow at each axial location x along the channel resembles the fully developed flow that would exist at that location if the channel shape did not vary with x; this is usually referred as the *lubrication approximation* [29,30]. The overall pressure drop is then calculated by integrating the local pressure gradient over the total length of the channel. Although good results can be obtained for creeping flow in mildly constricted channels, this method is not very accurate when the inertia effects become important or the amplitude of the constriction is substantial [26]. To obtain more accurate solutions, *asymptotic series solution* has been used by several authors for sinusoidal tubes [16,23–26] and two-dimensional channels with sinusoidal walls [22]. In this method, the solution of the Navier–Stokes equations is obtained by expanding the flow variables in powers of a small parameter characterizing the slowly varying character of the bounding walls, usually referred as *perturbation parameter*. Although the asymptotic solution method gives more accurate results compared to the lubrication approximation, the final solution for pressure drop and velocity field has a complex form even for simple cross-sectional geometries such as parallel plates or circular tubes.

Numerical and experimental methods are also used to investigate the laminar flow along slowly varying cross-section channels. Deiber and Schowalter [31] performed numerical study for the creeping flow through tubes with sinusoidal axial variations in diameter by using finite difference technique. The pressure drop results were then compared with those of measured through an independent experimentation. Hemmat and Borhan [32] used the boundary integral method to solve the Navier–stokes equations under the condition of creeping flow for axisymmetric capillary tubes whose diameter varies sinusoidally in the axial direction. Detailed velocity and pressure distributions within the capillary were obtained and the critical values of the geometrical parameters leading to flow reversal are reported.

As a result of recent advances in microfabrication techniques, microchannels with different cross-sectional geometries are fabricated for both commercial and scientific purposes. Finding analytical solutions for many practical cross-sections such as rectangle or trapezoid even for straight channels is complex and/or impossible.

* Corresponding author.
E-mail addresses: mohsen_akbari@sfu.ca, maa59@sfu.ca (M. Akbari).
URL: http://www.mohsenakbari.com (M. Akbari).

0017-9310/$ - see front matter © 2011 Elsevier Ltd. All rights reserved.
doi:10.1016/j.ijheatmasstransfer.2011.04.028

Nomenclature

a	major axis of ellipse/width of rectangle (m)	$Re_{\mathscr{L}}$	Reynolds number, $\rho U\mathscr{L}/\mu$ (–)
a_0	radius/width of the reference channel (m)	u	x-component of the velocity field (m/s)
A	local cross-sectional area (m^2)	U	local average velocity, Q/A (m/s)
A_0	cross-sectional area of the reference channel (m^2)	v	y-component of the velocity field (m/s)
b	minor axis of ellipse/height of rectangle (m)	w	z-component of the velocity field (m/s)
D_h	hydraulic diameter, $4A/\Gamma$ (m)		
f	fanning friction factor (–)	*Greek*	
I_p	polar momentum of inertia (m^4)	δ	maximum deviation from a_0 (m)
I_p^*	specific polar momentum of inertia, I_p/A^2 (–)	ϵ	aspect ratio, b/a (–)
L	channel length (m)	ε	perturbation parameter (–)
Q	volumetric flow rate (m^3/s)	Γ	local cross-sectional perimeter (m)
R	flow resistance, $\Delta p/Q$ (Pa s/m^3)	Γ_0	cross-sectional perimeter of the reference channel (m)
R_0	flow resistance of a reference straight channel, (Pa s/m^3)	$\mathscr{L}$	characteristic length scale (m)
R^*	dimensionless flow resistance, R/R_0 (–)	μ	viscosity (Pa s)
R_f^*	dimensionless frictional flow resistance (–)	ρ	density (kg/m^3)
R_i^*	dimensionless inertial flow resistance (–)	ξ	deviation parameter, δ/a_0 (–)

There are few works in the literature which are dealing with the hydrodynamics of laminar flow in slowly-varying channels of non-circular cross-section [2,27,28]. Lauga et al. [2] used the perturbation theory for creeping flow in channels constrained geometrically to remain between two parallel planes. Up to the first order accuracy of the perturbation solution, they showed that the velocity components perpendicular to the constraint plane cannot be zero unless the channel has both constant curvature and constant cross-sectional width. They only reported the zeroth order of the pressure gradient, which is identical to the lubrication approximation and only accounts for frictional effects. In another work, Gat et al. [28] studied the laminar incompressible gas flow through narrow channels with a variable cross-section using a higher order Hele–Shaw approximation [33]. Their method shows improvement over the classical Hele–Shaw solution [33], however, it does not account for the inertia effects that usually occurs in contractions or expansions. Wild et al. [27] used the perturbation theory to calculate the velocity and pressure distribution in an elliptical tube whose cross-sectional area varies slowly with a given profile along the axial direction. They [27] showed that the velocity distribution has a complicated form even up to the first order accuracy, but the local pressure gradient remains only a function of axial direction.

In the context of fluid flow in microchannels of arbitrary cross-section, few analytical studies have been performed for straight microchannels [34–36]. Yovanovich and Muzychka [34] showed that if the square root of cross-sectional area is used in the definition of the Poiseuille number, more consistent results can be obtained for various geometries. Zimmerman et al. [37] made an assessment of hydraulic radius, Saint–Venant, and Aissen's approximations to determine the hydraulic resistance of laminar fully developed flow in straight channels with irregular shapes. Comparing the proposed approximations with the available exact solutions, they showed that Saint–Venant, and Aissen's approximations are within 15% of the exact solution, whereas using the hydraulic radius can be in error by as much as 50%. Later, Bahrami et al. [35] introduced a general analytical model for the prediction of the Poiseuille number based on the square root of cross-sectional area in laminar fully developed flow along a straight microchannel of arbitrary cross-section. Using a "bottom-up" approach, they [35] showed that for constant fluid properties and flow rate in fixed cross-section channels, the Poiseuille number is only a function of geometrical parameters of the cross-section, i.e., cross-sectional perimeter, area, and polar moment of inertia. Their model was successfully validated against the numerical and experimental data for a wide variety of geometries including: hyperellipse, trapezoid, sine, square duct with two adjacent round corners, rhombic, circular sector, circular segment, annular sector, rectangular with semi-circular ends, and moon-shaped channels [35,38]. In a recent paper, Bahrami et al. [36] extended their general model to slip flow condition in a straight channel of arbitrary cross-section. Their model is shown to predict the numerical and experimental results obtained from the literature with good accuracy.

The purpose of this work is to develop an approximate method for the determination of the pressure drop of laminar, single-phase flow in slowly-varying microchannels of arbitrary cross-section by extending the previous models of Bahrami et al. [35] to slowly-varying microchannels of arbitrary cross-section. Starting from the solution of an elliptical cross-section [27], a generalized approximate model is proposed to compute the pressure drop in stream-wise periodic geometries, expansions and contractions. To verify the proposed model, an independent experimental investigation is carried out for stream-wise converging–diverging channels of rectangular cross-section with linear wall. Further validation is performed by comparing the results obtained from the present model and those obtained experimentally and numerically for a hyperbolic contraction of rectangular cross-section [21]. The proposed approach provides a powerful tool for basic designs, parametric studies, and the optimization analyses.

2. Model development

We seek a solution for steady-state laminar flow of a Newtonian fluid with constant properties in a slowly-varying conduit of arbitrary cross-section and wall profiles subjected to no-slip boundary condition on the walls. A schematic illustration of this channel is plotted in Fig. 1. Finding an exact analytical solution for such a problem is highly unlikely, but approximations can be obtained for a long channel in the form of a series in terms of a small perturbation parameter, ε. The idea is to take the advantage of the fact that variation in the direction of flow, x, is gradual compared to variation in the orthogonal directions; y and z. With ε is small, a regular perturbation expansion for both velocity and pressure fields can be written as [2]:

$$(u, v, w, p) = \sum_{n=0}^{\infty} \varepsilon^n (u_n, v_n, w_n, p_n), \tag{1}$$

where u, v, w are the velocity components and p is the pressure. The well-known perturbation approach [23–25] provides a method to

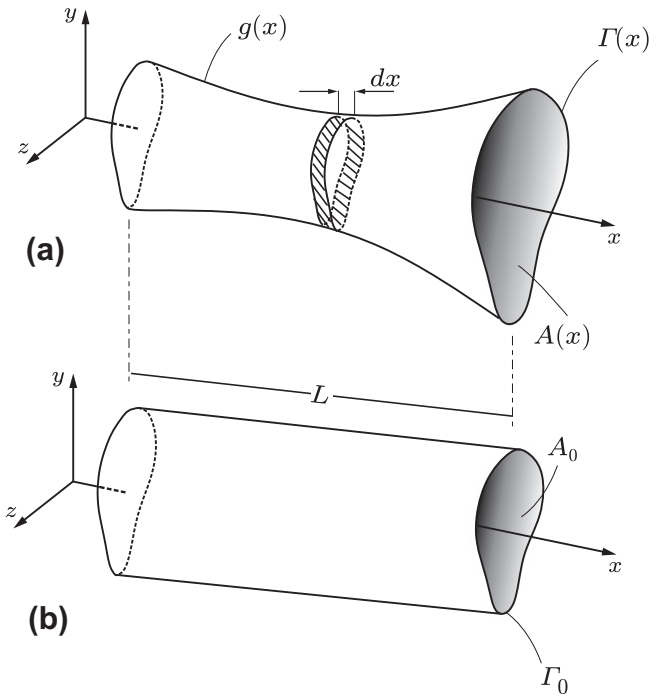

Fig. 1. (a) Schematic of a slowly-varying microchannel of arbitrary cross-section with a general wall profile of $g(x)$. (b) A reference straight channel with the cross-sectional area and perimeters of A_0 and Γ_0, respectively.

obtain the values of u_n, v_n, w_n and p_n by substituting Eq. (1) into the momentum and mass conservation equations. Finding u_n, v_n, w_n, and p_n, for the general case of three dimensional flows in arbitrary cross-section channels is impractical. Here, we use the perturbation solution of fluid flow in a slowly-varying tube of elliptical cross-section which is developed by Wild et al. [27] to propose a general model for arbitrary cross-section microchannels with a given wall profile. Elliptical cross-section is selected not because it is likely to occur in practice, but rather to utilize the unique geometrical property of its velocity solution.

Under the assumption of $\varepsilon^2 \ll 1$ where $\varepsilon = a_0/L; a_0$ is the hydraulic radius of a reference straight tube with the length of L, using the perturbation solution of Wild et al. [27], and after some rearrangements, the local pressure gradient for a slowly-varying conduit of elliptical cross-section can be obtained from the following relationship:

$$-\frac{1}{Q}\frac{dp}{dx} = \underbrace{\frac{4\mu[a^2(x)+b^2(x)]}{\pi a^3(x)b^3(x)}}_{\text{frictional}} - \underbrace{2\rho Q\left[\frac{dA(x)/dx}{A^3(x)}\right]}_{\text{inertial}}, \qquad (2)$$

$$A(x) = \pi a(x)b(x),$$

where $a(x)$ and $b(x)$ are the channel local half-major and half-minor axes, respectively; Q is the volumetric flow rate; $A(x)$ is the local cross-sectional area; $\mu$is the fluid viscosity; and $\rho$is the fluid density. For simplicity, we drop all (x) after this point. Noting Eq. (2), the followings can be concluded:

- The pressure gradient at each axial location can be obtained from the superposition of the frictional and the inertia terms.
- The frictional term in Eq. (2) resembles the laminar fully-developed flow in a straight channel of elliptical cross-section [39] and is a function of the major and minor axes of the ellipse. This is analogous to the lubrication approximation. One can follow the same steps introduced by Bahrami et al. [35] to obtain the local pressure gradient for slowly-varying microchannels of arbitrary cross-section.
- The inertia term only depends on dA/dx and the cross-sectional area but not the cross-sectional shape of the channel. In a converging channel, $dA/dx < 0$, the inertia term takes a positive value while for a diverging channel, $dA/dx > 0$, the inertia term is negative.
- The inertia term will vanish for any periodic profile, $dA(x)/dx = 0$. This is because the higher orders of the perturbation expansion are neglected, i.e., $\varepsilon^2 \ll 1$. It has been shown for simple geometries that the inertial pressure drop in a periodic channel will be non-negligible for sufficiently high Reynolds numbers or when the higher order terms in the perturbation expansion, i.e., Eq. (1), becomes significant [26,37].

Using Eq. (2), the local Poiseuille number based on an arbitrary length scale of $\mathscr{L}$ for slowly-varying microchannels of elliptical cross-section, $fRe_{\mathscr{L}}$, takes the following form:

$$fRe_{\mathscr{L}} = \left(\frac{\mathscr{L}}{\Gamma}\right)\left\{\underbrace{32\pi^2 I_p^*}_{\text{frictional}} - \underbrace{\frac{4\rho Q}{\mu}\left(\frac{dA/dx}{A}\right)}_{\text{inertial}}\right\}, \qquad (3)$$

where

$$fRe_{\mathscr{L}} = \frac{2}{\mu}\frac{(-dp/dx)}{Q}\left(\frac{\mathscr{L}}{\Gamma}\right)A^2, \qquad (4)$$

and

$$f = \frac{(-dp/dx)}{Q}\left(\frac{1}{1/2\rho U}\right)\left(\frac{A^2}{\Gamma}\right), \qquad (5)$$

$$Re_{\mathscr{L}} = \frac{\rho U \mathscr{L}}{\mu}, \qquad (6)$$

where U is the local average velocity, Γ is the local cross-sectional perimeter, and $I_p^* = I_p/A^2$ with $I_p = \int_A (y^2+z^2)dA$ is called the *specific polar moment of cross-sectional inertia* [35] and can be obtained from the following relationship for an elliptical cross-section:

$$I_p^* = \frac{1+\epsilon^2}{4\pi\epsilon}, \qquad (7)$$

where $0 < \epsilon \equiv b/a \leqslant 1$ is the aspect ratio of the channel cross-section such that the $\epsilon = 1$ leads to the circular cross-section. For other cross-sectional geometries such as rectangular, rhombic, trapezoidal, moon-shaped, triangular, circular segment, and annular sector, a comprehensive list of relationships can be found in Refs.[35,40].

Consistent with the model developed by Bahrami et al. [35] for straight microchannels of arbitrary cross-section, the present approximate model postulates that for constant fluid properties and flow rate in a variable cross-section channel, the local $fRe_{\mathscr{L}}$ for an arbitrary cross-section channel is only a function of the local specific polar momentum of cross-sectional area, $I_p^*, \mathscr{L}/\Gamma$ and the ratio of $(A^{-1}dA/dx)$.

Selection of the characteristic length scale is an arbitrary choice and will not affect the final solution. However, a more appropriate length scale leads to more consistent and similar results, especially when general cross sections are considered. For instance, a circular duct is fully described by its diameter; thus the obvious length scale is the diameter (or radius). For non-circular cross sections, the selection is not as clear. Possible length scales are: (i) the hydraulic diameter $D_h = 4A/\Gamma$, which has been conventionally used in many textbooks [39], (ii) effective radius defined as the average between the radius of largest inscribed circle and the radius of the circle with same area [41], (iii) the square root of the cross-sectional area,$\sqrt{A}$, which has been widely used for non-circular heat

conduction and convection problems [35,36,42,43], and (iv) the perimeter of the cross-section, Γ.

Fig. 2 shows the comparison of the frictional Poiseuille number for elliptical and rectangular cross-sections based on the hydraulic diameter, D_h, perimeter, Γ, and the square root of cross-sectional area, $\sqrt{A}$. It can be observed that the hydraulic diameter does not lead to a consistent trend for rectangular and elliptical cross-sections; the maximum difference is 30%. However, using either perimeter or the square root of cross-sectional area as the characteristic length scale leads to similar trends for the frictional Poiseuille number with the relative difference of less than 4% and 8%, respectively. Similar to the frictional Poiseuille number, the hydraulic diameter leads to a large relative differences between the inertial Poiseuille numbers of elliptical and rectangular cross-sections; the maximum relative difference is 24%. The square root of cross-sectional area leads to the relative difference of less than 11% between the inertial Poiseuille numbers of elliptical and rectangular cross-sections. However, when the cross-sectional perimeter is used as a characteristic length scale, Eq. (3) clearly shows that for constant fluid properties, flow rate, and geometrical parameters, there is no relative difference between the inertial Poiseuille numbers of the elliptical and rectangular cross-sections. These results suggest that using the cross-sectional perimeter as the characteristic length scale for overall Poiseuille number leads to better accuracies. Therefore, we use $\mathscr{L} = \Gamma$ through all our calculations. As a result, Eq. (3) reduces to:

$$fRe_\Gamma = 32\pi^2 I_p^* - \frac{4\rho Q}{\mu}\left(\frac{dA/dx}{A}\right). \tag{8}$$

It should be noted that one can convert the Poiseuille number based on different length scales using the following relationships:

$$\begin{aligned} fRe_{\sqrt{A}} &= \left(\frac{\sqrt{A}}{\Gamma}\right) fRe_\Gamma, \\ fRe_{D_h} &= \left(\frac{4A}{\Gamma^2}\right) fRe_\Gamma. \end{aligned} \tag{9}$$

For many applications, it is desired to calculate the total flow resistance of the channel. Using Eqs. (4) and (8) and integrating over the length of the channel, the total flow resistance of a slowly-varying microchannel of arbitrary cross-section, shown in Fig. 1, can be obtained from the following relationship:

$$R = \Delta p/Q = 16\pi^2\mu \int_{x_1}^{x_2} \frac{I_p^*}{A^2} dx + \rho Q\left(\frac{1}{A_2^2} - \frac{1}{A_1^2}\right), \tag{10}$$

where A_2^2 and A_1^2 are the microchannel cross-sectional area at x_1 and x_2 locations, respectively. It is beneficial to normalize the flow

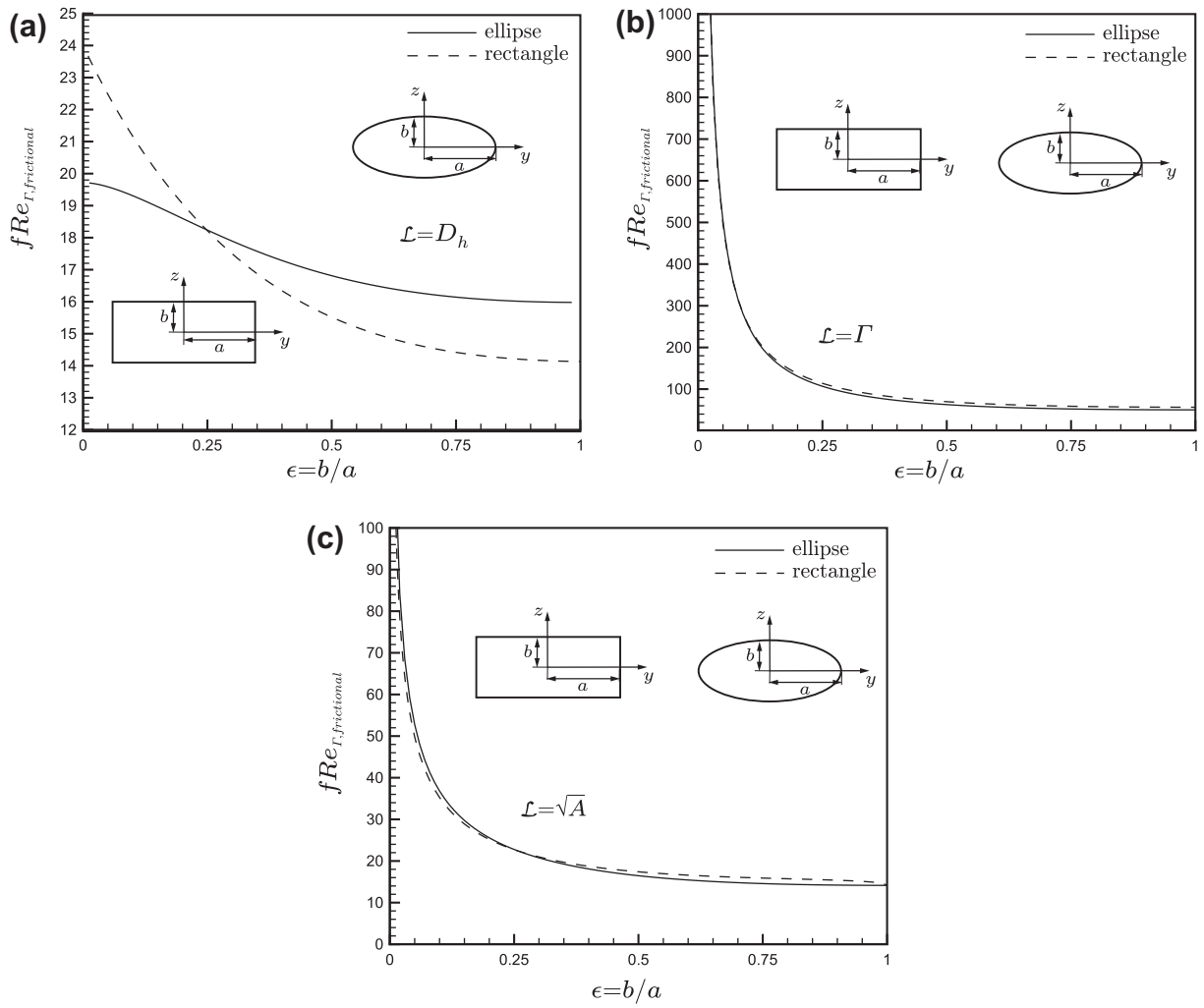

Fig. 2. Effect of the selection of (a) hydraulic diameter, D_h, (b) perimeter, Γ, and (c) square root of area, $\sqrt{A}$ as characteristic length scale on the relative difference between the frictional Poiseuille numbers of rectangular and elliptical cross-sections. The maximum differences are 30%, 8%, and 4%, for the hydraulic diameter, the square root of cross-sectional area, and the perimeter of cross-sectional area, respectively.

resistance with that of a straight reference channel with the specific polar momentum of inertia of $I^*_{p,0}$, length of L, and cross-sectional area of A_0. Thus:

$$R^* = R/R_0 = \underbrace{\int_{x_1^*}^{x_2^*} \frac{I_p^*/I_{p,0}^*}{A^{*2}} dx^*}_{R_f^*} + \underbrace{\frac{Re_{\Gamma_0}}{16\pi^2 I_{p,0}^*}\left(\frac{A_0/\Gamma_0}{L}\right)\left(\frac{1}{A_2^{*2}} - \frac{1}{A_1^{*2}}\right)}_{R_i^*}, \quad (11)$$

where $x^* = x/L, A_1^* = A_1/A_0$ and $A_2^* = A_2/A_0$. In Eq. (11), Γ_0 is the perimeter of the reference channel cross-section; $Re_{\Gamma_0} = \rho Q \Gamma_0/\mu A_0$; and R_0^* can be computed from the following relationship [35]:

$$R_0 = 16\pi^2 \mu \frac{I_{p,0}^*}{A_0^2} L. \quad (12)$$

Eq. (11) is a general relationship that accounts for both frictional and inertial effects on the flow resistance of fluid flow in slowly-varying microchannels of arbitrary cross-section. Dividing both sides of Eq. (11) by the frictional flow resistance, R_f^*, one obtains:

$$\frac{R^*}{R_f^*} = 1 + \frac{R_i^*}{R_f^*}. \quad (13)$$

Eq. (13) can be rearranged as follows:

$$\frac{R^*}{R_f^*} = 1 + \Phi Re_{\Gamma_0}. \quad (14)$$

The dimensionless parameter Φ appears in Eq. (14) is purely geometrical and defined as follows:

$$\phi = \frac{\left(\frac{1}{A_1^{*2}} - \frac{1}{A_2^{*2}}\right)}{16\pi^2 \int_{x_1}^{x_2} \frac{I_p^*}{A^{*2}} dx^*}\left(\frac{A_0/\Gamma}{L}\right) \quad (15)$$

Eq. (14) implies that the inertia term in a slowly-varying microchannel can be neglected under the following condition:

$$\Phi Re_{\Gamma_0} \ll 1. \quad (16)$$

3. Experimental procedure

3.1. Chemicals and materials

Distilled water was used as the testing liquid. SU-8 photoresist (Microchem, Newton, MA) and diacetone–alcohol developer solution (Sigma–Aldrich, St. Louis, MO) were used in the making of the positive relief masters by the procedure outlined below. Polydimethylsiloxane (PDMS) casts were prepared by thoroughly mixing the base and curing agent at a 10:1 ratio as per the manufacturer's instructions for the Sylgard 184 silicon elastomer kit (Dow Corning, Midland, MI).

3.2. Microfabrication

The PDMS/PDMS converging–diverging and reference straight microchannels were manufactured using the soft lithography technique [44]. Briefly, photomasks were designed by AutoCAD software (www.usa.autodesk.com) and printed with a 3500DPI printer (Island graphics Ltd., Victoria, BC). Masters containing the desired microchannel pattern have been made by spin coating of SU-8 negative photoresist on a glass slide to the desired nominal thickness. Both converging–diverging and reference channels were fabricated on the same master. Prior to the spin coating of SU-8, the glass slide was cleaned with isopropyl alcohol (IPA) and dried by high pressure air. The photoresist film was then hardened through a two-stage direct contact pre-exposure bake procedure (65 °C for 5 min and 95 °C for 30 min) and exposed to UV light for 100 s through the mask containing the channel pattern. A two stage post-exposure bake procedure (65 °C for 5 min, 95 °C for 30 min) was then used to enhance cross-linking in the exposed portion of the film. The slide was then placed in quiescent developer solution for 10 min to dissolve the unexposed photoresist, leaving a positive relief containing the microchannel pattern. Liquid PDMS was then poured over the master and exposed to vacuum condition (1 h) to extract all the bubbles in it and cured at 85 °C for 15 – 20 min yielding a negative cast of the microchannel pattern. An enclosed microchannel was then formed by bonding the PDMS cast with another piece of PDMS via plasma treatment. Each variable cross-section microchannel contained ten converging–diverging modules with linearly varying wall with the module length of 3 mm ± 0.02 mm.

Dimensions of the channel were measured by an image processing method described in [38]. Briefly, an inverted microscope (Unitron, Commack, NY) equipped with 5 X, 0.12 N.A. and 10 X, 0.4 N.A. objectives and a CCD camera was used. The low magnification objective was used to measure the length of each module. Images of the channels were taken at three different locations and then imported into an image processing software (Zarbco video toolbox, Ver. 1.65), which was calibrated with an optical ruler (Edmund optics, Barrington, NJ), to measure the in-plane geometrical parameters. For each microchannel, average values are reported. To determine the channel depth, the pressure drop along each straight reference channel was measured using the method described later and Eq. (12) with constant geometrical parameters was used to compute the channel depth. The geometrical parameters are reported in Table (1).

3.3. Experimental procedure

Schematic diagram of the experimental setup is depicted in Fig. 3. Controlled measurements of the flow resistance for flow through a microchannel were performed using a syringe pump (Harvard Apparatus, Quebec, Canada) with Hamilton Gastight glass syringes, which provides a constant flow rate with the accuracy of ±0.5%. A range of Reynolds number from $Re_{\Gamma_0} = 10 - 75$ (corresponding Reynolds number based on the hydraulic diameter falls in the range of 2 – 15) was covered by changing the volumetric flow rate from 30 L/min to 100 μL/min.The accuracy of the nominal flow rate was independently evaluated by weighting the collected water over the elapsed time. It was observed that the relative difference between the measured and nominal flow rate was less than 4% in our experiments. This value is taken as the uncertainty in the flow rate readings. The pressure drop along the flow channel was measured using a gauge pressure transducer (Omega Inc., Laval) with the accuracy of ±0.004 psi (±30 Pa) and a nominal pressure range of 0 – 5 psi. This pressure sensor was connected to the entrance of the microchannel using a 1 cm-long piece of plastic tubing with an inner diameter of 3 mm. From the exit of the microchannel, 2 cm of the same kind of plastic tubing released the fluid into a waste container at atmospheric pressure. The contribution of the connecting tube is calculated to be less than 0.01% of the total measured pressure drop. Measured pressure was monitored and recorded with a computerized data acquisition system (Labview 8.5, National Instrument, www.ni.com). The flow was considered to have reached a steady state condition when the readings of the pressure drop did not change with time. Due to the fluctuations of the volumetric flow rate provided by the syringe pump and formation of the droplets at the tube exit, periodic pressure fluctuations were observed in the pressure vs. time graph, even for the steady-state condition. Average values of these fluctuations are considered in this experiment. For a given channel, the measurement of pressure drop was repeated three times for each

Table 1
Experimental parameters in present work.

Channel #	$2a_0$ (μm)	$2b$ (μm)	$D_{h,0}$ (μm)	Γ_0 (μm)	L (mm)	$\epsilon_0 = b/a_0$	$\xi = \delta/a_0$
1	311	78	125	780	3	0.25	0.27
2	286	93	140	760	3	0.32	0.42
3	283	62	103	691	3	0.22	0.53
4	389	36	66	850	3	0.09	0.09
5	286	63	104	700	3	0.22	0.42

$Q = 30 - 100$ μL/min; $\Delta p = 0.86 - 24.13$ kPa.

flow rate to ensure the reproducibility of the results. An arithmetic averaging method [45] was performed to determine the final results. The maximum difference between the averaged and the actual values was observed to be less than 1.5%. In this experiment the effects of the developing length, minor losses, viscous heating and channel deformation were neglected [38]. The experimental values of R_f^* were computed from the following relationship:

$$R^*_{\text{exp}} = \frac{(\Delta p/Q)}{(\Delta p/Q)_0}, \tag{17}$$

where the parameters with "0" subscript correspond to the measured flow resistance of the reference straight channel. The uncertainty associated with the measured R^*_{exp} is calculated from the following relationship [45]:

$$\frac{\psi_{R^*}}{R^*} = \left[\left(\frac{\psi_{\Delta p}}{\Delta p}\right)^2 + \left(\frac{\psi_Q}{Q}\right)^2\right]^{1/2}, \tag{18}$$

where ψ_{R^*}/R^* is the relative uncertainty of the dimensionless flow resistance, $\psi_{\Delta p}$ is the uncertainty associated with the pressure measurement is ±0.25% of the full scale, i.e., ±30 Pa, and ψ_Q is the uncertainty associated with the flow rate provided by the syringe pump with $\psi_Q/Q = \pm 0.04$. The calculated uncertainties are reported as error bars in the experimental results.

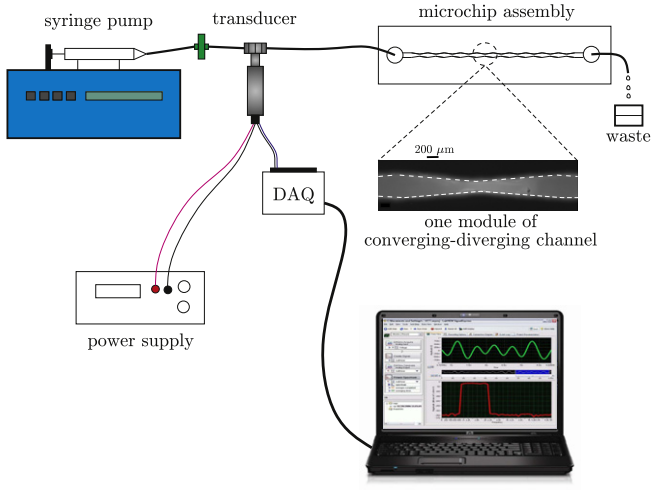

Fig. 3. Schematic diagram of the experimental setup for pressure measurements in converging–diverging channels. The inert in the module of converging–diverging channel is Rhodamine B, for clarity.

4. Results and discussion

In this section, the present model is compared against the experimental data obtained in this work for stream-wise periodic channels of rectangular cross-section and numerical and experimental data collected from the work of Oliveira et al. [21] for a hyperbolic contraction.

The converging–diverging channels were fabricated with a linear wall profile defined as follows, see Fig. 4(a):

$$a^* = a(x^*)/a_0 = \begin{cases} [1 - \xi(4x^* + 1)], & -1/2 \leqslant x^* \leqslant 0, \\ [1 + \xi(4x^* - 1)], & 0 \leqslant x \leqslant 1/2, \end{cases} \tag{19}$$

where the origin is located at the channel throat, a^* is the channel with normalized with respect to the staight reference channel with the with of a_0; $x^* = x/L$ is the normalized coordinate in the axial dimention with respect to the module lenght of L; $\xi = \delta/a_0$is the *deviation parameter* which shows the amount of deviation from a straight channel with the average width of a_0. For such a geometry, the inertia term in Eq. (11) is eliminated because $A_2^* = A_1^*$. Specific polar moment of inertia for a rectangular cross-section microchannel can be obtained from Ref. [40]; thus one can calculate the ratio of $I_p^*/I_{p,0}^*$ as follows:

$$I_p^*/I_{p,0}^* = \frac{a^* + \epsilon_0^2}{a^*(1 + \epsilon_0^2)}, \tag{20}$$

where similar to an elliptical cross-section channell, $\epsilon = b/a$, is the local channel aspect ratio, $\epsilon_0 = b/a_0$ is the aspect ratio of the straight reference channel, and a. Dimensionless cross-sectional area for a rectangular cross-section can be obtained from the following relationship:

$$A^* = a^*, \tag{21}$$

where the ratio of a/a_0 can be obtained from Eq. (19). Substituting Eqs. (21) and (20) into Eq. (11) gives:

$$R^* = \int_{-1/2}^{1/2} \frac{a^* + \epsilon_0^2}{1 + \epsilon_0^2} dx^*, \tag{22}$$

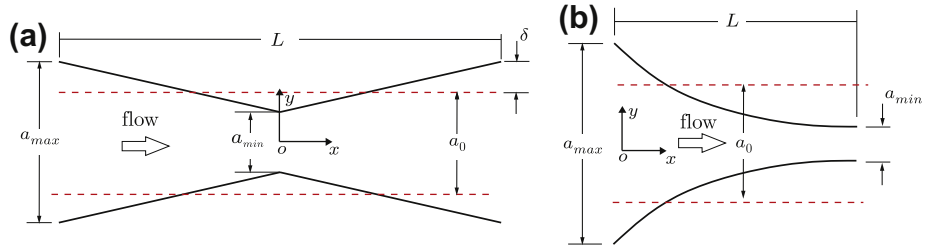

Fig. 4. Schematic of the studied wall geometries: (a) stream-wise periodic wall with linear profile and (b) hyperbolic contraction.

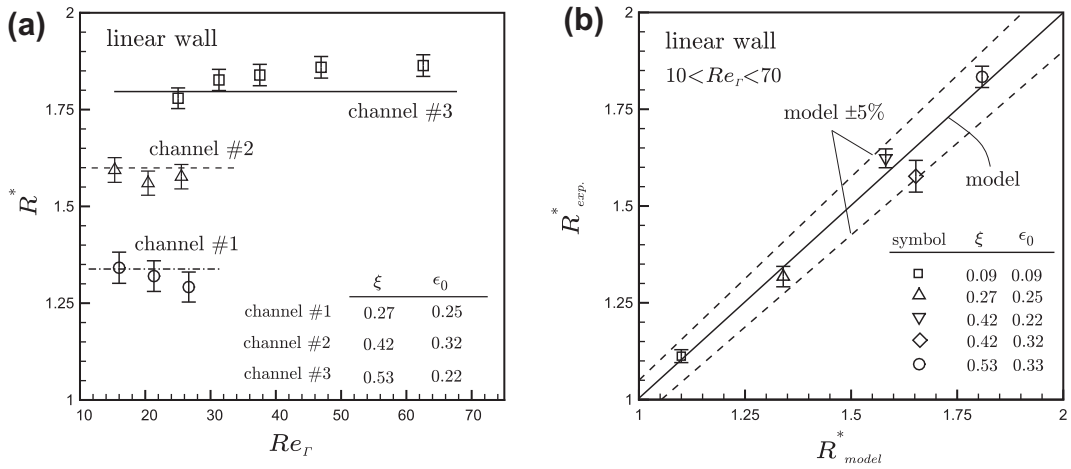

Fig. 5. Experimental data for stream-wise periodic geometry with linear wall: (a) variation of the data with respect to the Reynolds number, the symbols are the experimental data and the lines represent the values predicted by Eq. (23); (b) experimental data vs. proposed model. Each symbol corresponds to one channel, the solid line shows the proposed model and the dashed lines are model ±5%. Note that the range of Reynolds number based on the hydraulic diameter is less than 15.

Integrating Eq. (22) and after some simplifications, the dimensionless flow resistance of a rectangular microchannel cross-section with a linear wall profile can be obtained from the following relationship:

$$R^* = \frac{2\xi\epsilon_0^2 + (1-\xi^2)^2 \ln\left(\frac{1+\xi}{1-\xi}\right)}{2\xi(1-\xi^2)^2(1+\epsilon_0^2)}. \tag{23}$$

Fig. 5(a) shows the variation of experimental data for R_f^* with Reynolds number. For clarity, the results are only plotted for three samples. The geometrical parameters for each channel are shown in the plot. In agreement with the proposed theory, the trend of data shows that R_f^* is an independent function of the Reynolds number. Thus for each microchannel, the average value of R^* over the Reynolds number is taken and plotted against the values obtained from the compact relationship of Eq. (23) in Fig. 5(b). Good agreement between the model and experimental results can be observed.

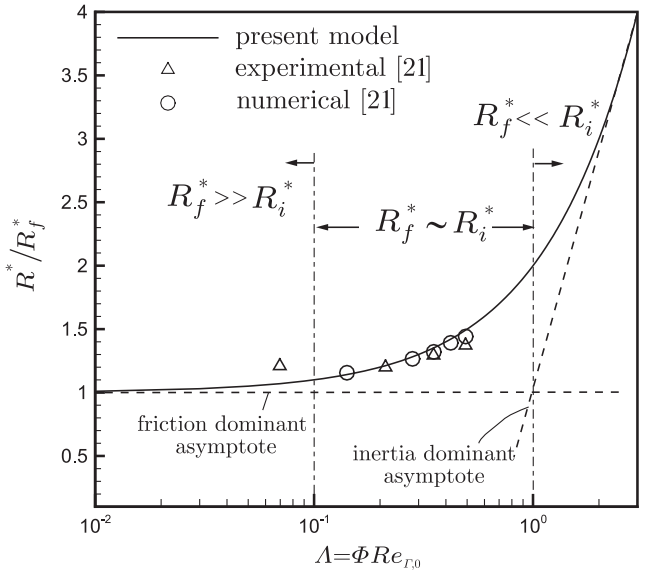

Fig. 6. Comparison of the theoretical model to experimental and numerical results from Oliveira et al. [21]. The solid line corresponds to the proposed model, Eq. (25) which includes both frictional and inertia terms, and delta (△) and circular (○) symbols are the experimental and numerical data, respectively. Two asymptotes of friction dominant and inertia dominant regions are shown in the plot by dashed lines.

A hyperbolic contraction as shown in Fig. 4(b) is defined as follows:

$$a^* = a(x^*)/a_{\max} = \frac{1}{1+(\beta-1)x^*}, \tag{24}$$

where a^* is the channel with normalized with respect to the maximum width of $a_{\max}$; $\beta = a_{\max}/a_{\min}$; $a_{\min}$ is the minimum width of the channel; and L is the channel length. For such a geometry, both frictional and inertia terms exist. Following the same steps explained for the linearly varying wall microchannel the total dimensionless flow resistance can be obtained from the following compact relationship:

$$R^* = \frac{\left[2(\beta-1)^2 + (\beta^2+1)(\epsilon_0 \ln\beta)^2\right](\beta+1)\ln\beta}{4(\beta-1)^2(1+\epsilon_0^2)} + \frac{3(\beta+1)(\ln\beta)^2\epsilon_0\sqrt{\epsilon_0}}{16\pi^2(\beta-1)(1+\epsilon_0^2)(1+\epsilon_0)^2} Re_{\Gamma_0}\varepsilon. \tag{25}$$

Fig. 6 shows the comparison between the experimental and numerical data obtained by Oliveira et al. [21] for a hyperbolic contraction defined by Eq. (24) with rectangular cross-section and the proposed model, Eq. (14). The geometrical and flow conditions used by Oliveira et al. [21] are listed in Table (2). The present model illustrates good agreement with the data; the relative difference between the data and the compact relationship of Eq. (25) is less than 8%. Three regions can be identified in Fig. 6 based on the value dimensionless parameter $\Lambda = \Phi Re_{\Gamma_0}$:

(i) Friction dominated, $\Lambda \ll 1$, the flow is purely frictional and the lubrication theory gives accurate prediction of the pressure drop.
(ii) Transitional, $\Lambda \sim O(1)$, both frictional and inertial effects should be taken into account.
(iii) Inertia dominated, $\Lambda \gg 1$, the inertial effect is dominant, thus the effect of wall profile becomes negligible and the flow resistance can be obtained by computing the cross-section geometrical parameters for the reference channel,

Table 2
Geometrical and flow conditions used for the hyperbolic contraction.

Parameter	$a_{\max}$ (μm)	$a_{\min}$ (μm)	b (μm)	Γ_0 (μm)	L (μm)	ϵ_0	β	$Re_{\Gamma,0}$
Value	400	19.9	46	217	382	0.7	20.1	20–160

inlet and outlet cross-sectional area, and the Reynolds number, see Eq. (11).

As an example, the data obtained from [21] fall in the transitional region which means that considering the lubrication approximation will lead to an underprediction of the pressure drop. One should note that for a stream-wise periodic geometry, the inlet and outlet cross-sectional areas for one module are the same, thus $\Lambda = 0$ and the inertial effect through the entire module of a converging–diverging channel becomes negligible.

5. Summary and conclusions

The pressure drop of single phase flow in slowly-varying microchannels of arbitrary cross-section has been investigated in this study. Starting from the available perturbation solution of an elliptical cross-section and assuming that the second and higher order perturbation terms are negligible, a general approximate model has been developed. The proposed model presents improved accuracy over the lubrication approximation by taking the inertial effect into account. An independent experimental study has been conducted for microchannels with stream-wise periodic geometry and rectangular cross-section. Experimental results have been used to verify the proposed model. Further validation is performed by comparing the model with the numerical and experimental data collected from the literature for a hyperbolic contraction. The highlights of this study are as follows:

- Selection of the characteristic length scale does not affect the flow regime or pressure drop. Using the cross-sectional perimeter or square root of area as a characteristic length scale in the definition of the Poiseuille number leads to a more consistent trend between different cross-sections. Since the cross-sectional perimeter gives better accuracy, it has been used as the characteristic length scale through our analysis.
- For a slowly-varying microchannel of arbitrary cross-section, the Poiseuille number of laminar flow of a fluid with constant properties can be obtained from the superposition of frictional and inertial terms. A dimensionless parameter is introduced to determine the importance of each term.
- Comparison with experimental and numerical results shows good agreement between the proposed model and the collected data. It has been observed that for a hyperbolic contraction, using the lubrication approximation underestimates the pressure drop. However, taking the inertia term into account by the proposed model gives excellent improvement over the lubrication approximation.

Acknowledgments

The authors gratefully acknowledge the financial support of the Natural Sciences and Engineering Research Council of Canada (NSERC), BC Innovation Council (BCIC), Canada Research Chair Program, and K. Wong's assistance in experimental setup design and pressure measurements.

References

[1] A. Stroock, S. Dertinger, A. Ajdari, I. Mezic, H. Stone, G. Whitesides, Chaotic mixer for microchannels, Science 295 (5) (2002) 647–651.
[2] E. Lauga, A. Stroock, H. Stone, Three-dimensional flows in slowly varying planar geometries, Phys. Fluids 16 (2004) 3051–3063.
[3] S. Hsieh, Y. Huang, Passive mixing in micro-channels with geometric variations through μPIV and μLIF measurements, J. Micromech. Microeng. 18 (2008) 065017.
[4] R. Liu, K. Sharp, M. Olsen, M. Stremler, J. Santiago, R. Adrian, H. Aref, D. Beebe, A passive three-dimensional C-shapehelical micromixer, J. Microelectromech. Syst. 9 (2) (2000) 190–198.
[5] A. Bertsch, S. Heimgartner, P. Cousseau, P. Renaud, Static micromixers based on large-scale industrial mixer geometry, Lab Chip 1 (1) (2001) 56–60.
[6] X. Xuan, B. Xu, D. Li, Accelerated particle electrophoretic motion and separation in converging–diverging microchannels, Anal. Chem. 77 (14) (2005) 4323–4328.
[7] X. Xuan, D. Li, Particle motions in low-Reynolds number pressure-driven flows through converging–diverging microchannels, J. Micromech. Microeng. 16 (2006) 62–69.
[8] E. Sparrow, A. Prata, Numerical solutions for laminar flow and heat transfer in a periodically converging–diverging tube, with experimental confirmation, Numer. Heat Transfer A. Appl. 6 (4) (1983) 441–461.
[9] G. Wang, S. Vanka, Convective heat transfer in periodic wavy passages, Int. J. Heat Mass Transfer 38 (17) (1995) 3219–3230.
[10] T. Nishimura, Y. Bian, Y. Matsumoto, K. Kunitsugu, Fluid flow and mass transfer characteristics in a sinusoidal wavy-walled tube at moderate Reynolds numbers for steady flow, Heat Mass Transfer 39 (3) (2003) 239–248.
[11] A. Lahbabi, H. Chang, Flow in periodically constricted tubes: transition to inertial and nonsteady flows, Chem. Eng. Sci. 41 (10) (1986) 2487–2505.
[12] A. Payatakes, C. Tien, R. Turian, A new model for granular porous media: part I. Model formulation, AIChE J. 19 (1) (1973) 58–67.
[13] Y. Bernabé, J. Olson, The hydraulic conductance of a capillary with a sinusoidally varying cross-section, Geophys. Res. Lett. 27 (2) (2000) 245–248.
[14] A. Tamayol, M. Bahrami, Analytical determination of viscous permeability of fibrous porous media, Int. J. Heat Mass Transfer 52 (9–10) (2009) 2407–2414.
[15] A. Tamayol, M. Bahrami, In-plane gas permeability of proton exchange membrane fuel cell gas diffusion layers, J. Power Sources 196 (2010) 3559–3564.
[16] J. Forrester, D. Young, Flow through a converging–diverging tube and its implications in occlusive vascular disease–II: theoretical and experimental results and their implications, J. Biomech. 3 (3) (1970) 307–310.
[17] D. Ross, L. Locascio, Microfluidic temperature gradient focusing, Anal. Chem. 74 (11) (2002) 2556–2564.
[18] G. Sommer, Electrokinetic Gradient-Based Focusing Mechanisms for Rapid, On-Chip Concentration and Separation of Proteins, University of Michigan, 2008.
[19] S. Kim, G. Sommer, M. Burns, E. Hasselbrink, Low-power concentration and separation using temperature gradient focusing via Joule heating, Anal. Chem. 78 (23) (2006) 8028–8035.
[20] D. James, G. Chandler, S. Armour, A converging channel rheometer for the measurement of extensional viscosity, J. Non-Newton. Fluid Mech. 35 (2–3) (1990) 421–443.
[21] M. Oliveira, M. Alves, F. Pinho, G. McKinley, Viscous flow through microfabricated hyperbolic contractions, Exp. Fluids 43 (2) (2007) 437–451.
[22] P. Kitanidis, B. Dykaar, Stokes flow in a slowly varying two-dimensional periodic pore, Transport Porous Med. 26 (1) (1997) 89–98.
[23] M. Manton, Low Reynolds number flow in slowly varying axisymmetric tubes, J. Fluid Mech. 49 (3) (2006) 451–459.
[24] J. Chow, K. Soda, Laminar flow in tubes with constriction, Phys. Fluids 15 (1972) 1700–1717.
[25] M. Van Dyke, Slow variations in continuum mechanics, Adv. Appl. Mech. 25 (1987) 1–45.
[26] S. Sisavath, X. Jing, R. Zimmerman, Creeping flow through a pipe of varying radius, Phys. Fluids 13 (2001) 2762–2772.
[27] R. Wild, T. Pedley, D. Riley, Viscous flow in collapsible tubes of slowly varying elliptical cross-section, J. Fluid Mech. 81 (2) (1977) 273–294.
[28] A. Gat, I. Frankel, D. Weihs, A higher-order Hele–Shaw approximation with application to gas flows through shallow micro-channels, J. Fluid Mech. 638 (2009) 141–160.
[29] M. Akbari, D. Sinton, M. Bahrami, Laminar fully developed flow in periodically converging–diverging microtubes, Heat Transfer Eng. 31 (8) (2010) 628–634.
[30] S. Sisavath, A. Al-Yaaruby, C. Pain, R. Zimmerman, A simple model for deviations from the cubic law for a fracture undergoing dilation or closure, Pure Appl. Geophys. 160 (5) (2003) 1009–1022.
[31] J. Deiber, W. Schowalter, Flow through tubes with sinusoidal axial variations in diameter, AIChE J. 25 (4) (1979) 638–645.
[32] M. Hemmat, A. Borhan, Creeping flow through sinusoidally constricted capillaries, Phys. Fluids 7 (1995) 2111.
[33] G. Batchelor, An Introduction to Fluid Dynamics, Cambridge University Press, 2000.
[34] M. Yovanovich, Y. Muzychka, Solutions of Poisson equation within singly and doubly connected prismatic domains, in: 1997 National Heat Transfer Conference, Baltimore, MD, 1997.
[35] M. Bahrami, M. Michael Yovanovich, J. Richard Culham, A novel solution for pressure drop in singly connected microchannels of arbitrary cross-section, Int. J. Heat Mass Transfer 50 (13–14) (2007) 2492–2502.
[36] M. Bahrami, A. Tamayol, P. Taheri, Slip-flow pressure drop in microchannels of general cross section, J. Fluids Eng. 131 (2009) 031201–031208.
[37] R. Zimmerman, A. Al-Yaarubi, C. Pain, C. Grattoni, Non-linear regimes of fluid flow in rock fractures, Int. J. Rock Mech. Min. Sci. 41 (3) (2004) 384.
[38] M. Akbari, D. Sinton, M. Bahrami, Pressure drop in rectangular microchannels as compared with theory based on arbitrary cross section, ASME J. Fluids Eng. 131 (2009) 041202-1–041202-8.
[39] F. White, Viscous Flow, McGraw-Hill Inc, 1991.

[40] M. Bahrami, M. Yovanovich, J. Culham, et al., Pressure drop of fully-developed, laminar flow in microchannels of arbitrary cross-section, J. Fluids Eng. 128 (2006) 1036–1044.
[41] S. Bryant, P. King, D. Mellor, Network model evaluation of permeability and spatial correlation in a real random sphere packing, Transport Porous Med. 11 (1) (1993) 53–70.
[42] M. Yovanovich, A general expression for predicting conduction shape factors, AIAA Prog, in Astro, and Aeronautics: Thermophysics and Spacecraft Thermal Control, vol. 35, 1974, pp. 265–291.
[43] Y. Muzychka, M. Yovanovich, Laminar flow friction and heat transfer in non-circular ducts and channels: part I – hydrodynamic problem, in: Proceedings of Compact Heat Exchangers, A Festschrift on the 60th Birthday of Ramesh K. Shah, Grenoble, France, 2002, pp. 123–130.
[44] J. McDonald, D. Duffy, J. Anderson, D. Chiu, H. Wu, O. Schueller, G. Whitesides, Fabrication of microfluidic systems in poly (dimethylsiloxane), Electrophoresis 21 (1) (2000) 27–40.
[45] J. Holman, W. Gajda, Experimental Methods for Engineers, McGraw-Hill, New York, 1994.